Carbon composite membrane derived from MIL-125-NH_2 MOF for the enhanced extraction of emerging pollutants

Neus Crespí Sánchez,[a] *Jorge Luis Guzmán-Mar,*[b] *Laura Hinojosa-Reyes,*[b] *Gemma Turnes Palomino,**[,a] *Carlos Palomino Cabello**[,a]

[a] *Department of Chemistry, University of the Balearic Islands, Palma de Mallorca, E-07122, Spain.*

[b] *Universidad Autónoma de Nuevo León, UANL, Facultad de Ciencias Químicas, Cd. Universitaria, Pedro de Alba s/n, C.P. 66455. San Nicolás de los Garza, Nuevo León, México.*

**E-mail: carlos.palomino@uib.es *E-mail: g.turnes@uib.es Fax: (+34) 971 173426 Phone: (+34) 971 173389*

ABSTRACT

Porous carbon derived from amine-functionalized MIL-125 metal-organic framework (C-MIL-125-NH_2) was prepared by carbonization at high temperature under inert atmosphere, and used for adsorption of bisphenol A (BPA) and 4-tert-butylphenol (4-tBP). The obtained carbon showed bimodal porosity and fast extraction of both pollutants in batch conditions following a pseudo-second-order model. The adsorption mechanism was studied by the measurement of zeta potential, and the results suggested that π-π stacking interactions between the carbon material and the phenol molecules probably are the main sorption mechanism. The prepared C-MIL-125-NH_2 was incorporated into mechanically stable membranes for flow-through solid-phase extraction of studied phenols prior to HPLC analysis. The hybrid material showed excellent permeance to flow, easy regeneration and good performance for the simultaneous enrichment of mixtures of BPA and 4-tBP, facilitating their determination when present at low concentration levels.

Keywords: Metal-organic frameworks, porous carbons, membranes, solid-phase extraction, water pollutants.

1. Introduction

Water contamination derived from emerging pollutants such as antibiotics, pesticides, food additives and other organic pollutants has adverse effects on human health, and is a worldwide environmental problem (Chong et al., 2010; Rivera-Utrilla et al., 2013). Emerging pollutants are any synthetic or naturally compound with potentially toxic ecological and endocrine-disrupting effects that have recently been introduced in environment and still remain unregulated (Dhaka et al., 2019; Freyria et al., 2018; Rivera-Utrilla et al., 2013). Different strategies have been developed for the remediation of wastewater such as ultrasonic degradation (Chu et al., 2017), Fenton oxidation (Wang et al., 2015), photocatalysis (Zhang et al., 2018) and adsorption (Hasan and Jhung, 2015). Among them, the use of porous materials as sorbents for pollutant extraction, due to its simplicity, selectivity and efficiency, has gained great interest and is being widely studied (Poole, 2003; Wu and Zhao, 2011).

Based on their high chemical and thermal stability, aromatic structure and large surface area, carbon-based materials have been explored as sorbents for the extraction of emerging pollutants (Joseph et al., 2011; Pan et al., 2008; Park et al., 2015). Over recent decades, different synthetic procedures have been developed in order to prepare novel porous carbon structures with hierarchical porosity and new properties, among which stands out the template method, which consists on the preparation of an organic/inorganic template composite followed by the carbonization and removal of the inorganic template (Lee et al., 2006). Due to their high surface area, tunable pore sizes, and chemical variability, metal-organic frameworks (MOFs), formed by linking metal ions or clusters with multidentate organic ligands (Cui et al., 2016; Meek et al., 2011; Rowsell and Yaghi, 2004), have been considered as potential precursors to synthesize nanoporous carbon materials (Chaikittisilp et al., 2013; Liu et al., 2010). By MOF carbonization at high temperature under inert atmosphere, organic linkers are converted to a porous

carbon structure, while the metallic component is distributed in this carbonaceous structure shaped like metal or metal oxide nanoparticles.

Recently, among the different types of MOFs, MIL-125 (*Materials Institute Lavoisier*), based on the coordination of titanium clusters with aromatic carboxylic acids, has been used as precursor to obtain different nanoporous carbons. Due to their excellent anode characteristics, these porous carbons have been widely studied as materials for rechargeable lithium ion batteries (An et al., 2017; Shi et al., 2017; Wang et al., 2015). Other examples of application of MIL-125-derived carbons are focused on the photocatalytic degradation of different toxic compounds (Guo et al., 2014; Li et al., 2018) and on microwave absorption (Ma et al., 2017). However, the potential of the porous carbons derived from MIL-125 as sorbents for removal of pollutants has not been widely explored.

For practical extraction applications, the direct use of porous materials is limited by the hard and laborious recovery of the sorbent from the sample medium. In this regard, an interesting alternative to solve this limitation is the positioning of the porous sorbents on functional supports, which facilitates their applicability for the extraction of pollutants from water. Among the different supports used, the preparation of composites based on membranes has gained increasing interest for the removal of organic pollutants because of their easy regenerability and outstanding flow-through properties. For instance, nanofiltration membranes were prepared with functionalized halloysite nanotubes for the extraction of Direct Red 28 dye (Zeng et al., 2016). UiO-66, MIL-101 and ZIF-8 MOFs have also been used for the preparation of different membranes, which have demonstrated their potential for the extraction of phenols (Ghani et al., 2017), phthalate esters (Wang et al., 2015) and progesterone (Ragab et al., 2016), respectively, while poly(vinyl alcohol)/poly(acrylic acid) membranes have been studied for the extraction of various dyes (Yan et al., 2015).

The aim of this work is to explore the use of a porous carbon, derived from amine-functionalized MIL-125 MOF (C-MIL-125-NH_2), membrane as functional support for the extraction and preconcentration of bisphenol A (BPA) and 4-tert-butylphenol (4-tBP). These pollutants have been closely studied in recent years because they have shown estrogenic effects in fish, avian, and mammalian cells and are suspected of having endrocrine-disrupting toxicity (Li et al., 2005). After batch extraction experiments with C-MIL-125-NH_2 material, and in order to improve the applicability of the obtained porous carbon, a hybrid membrane was prepared using a nylon filter as support and polyvinylidene fluoride (PVDF) as binder, characterized and tested for the extraction and preconcentration of BPA and 4-tBP. Experimental parameters involved in the extraction process such as pH, sample volume and recyclability have been evaluated.

2. Experimental

2.1. Chemicals

Acetonitrile (HPLC, > 99.8%), Methanol (≥99.8%), acetone (≥99.8%), and N,N-dimethylformamide (DMF, 99.5%), and hydrochloric acid (HCl, 37.0%) were obtained from Scharlau. Titanium (IV) isopropoxide (≥99.8%) and 2-aminoterephthalic acid (99%) were acquired from ACROS. Bisphenol A (BPA, 97%), 4-tert-butylphenol (4-tBP, 99%), sodium hydroxide (NaOH, ≥97.0%) and polyvinylidene difluoride (PVDF, MW ~ 180,000) were obtained from Aldrich. GVS Maine Magna 0.45 μm Nylon filters of 25 mm diameter were used as initial supports.

The working solutions were obtained by mixing the desired volume of stock solution of each selected phenol (1000 mg L^{-1}) and diluting to the appropriate volume with water. All solutions were prepared using Milli-Q water (Direct-8 purification system, resistivity > 18 MΩ, Millipore Iberica, Spain).

2.2. *Instrumentation*

Powder XRD data were collected by using CuK_α radiation on a Bruker D8 Advance diffractometer. Thermogravimetric analysis (TGA) was carried out in an air atmosphere using a TA Instrument SDT 2960 simultaneous DSC-TGA. Nitrogen adsorption isotherms were measured at 77 K by using a TriStar II (Micromeritics) gas adsorption analyzer. The samples were previously outgassed at 393 K overnight. The data of the isotherms were analyzed by using the Brunauer-Emmett-Teller (BET) method to determine the specific surface area and the two dimensional non local density functional theory (2D-NLDFT) model for the determination of pore volume and pore size distribution. The morphology and elemental distribution of the prepared materials were analyzed by using a scanning electron microscope (SEM) Hitachi S-3400N, equipped with a Bruker AXS Xflash 4010 energy-dispersive X-ray spectroscopy (EDS) system, and a transmission electron microscope Hitachi ABS operated at 100 kV. Zeta potential was measured by employing a Zetasizer Nano ZS90 (Malvern). In batch experiments the absorbance measurements were carried out using a HP 8453 UV-vis spectrophotometer. Phenols in the collected filtrates were analyzed by reversed phase high-performance liquid chromatography (HPLC). Chromatographic experiments were performed by using a Jasco HPLC instrument composed of a high-pressure pump (PU-4180), a manual injector, and a UV/Vis diode array detector (MD-4017). The separation of phenol compounds was performed at room temperature on a Phenomenex Kinetex EVO C_{18} 100A core-shell column (150 mm x 4.6 mm i.d. 5 μm) with a guard column (5 mm x 4.6 mm i.d.). The mobile phase was acetonitrile:water (50:50, v/v) at a flow rate of 1 mL min^{-1}. The detection wavelength was 225 nm.

2.3. *Synthesis of MIL-125-NH_2*

Titanium based MIL-125-NH_2 was synthesized by microwave heating according to a procedure described in a previous report (Kim et al., 2013). Typically, 0.54 mL of titanium isopropoxide were added under constant stirring to 0.60 g of 2-aminoterephthalic acid dissolved in 30 mL of a mixture of

dimethylformamide (DMF) and methanol (1:1, v/v). After 5 min of additional stirring, the mixture was introduced into the Teflon liner of an autoclave and heated at 423 K for 1 h in a microwave oven (Stard D, Milestone). Finally, the obtained yellow solid was filtered and washed thoroughly with DMF and methanol.

2.4. Synthesis of MOF-derived carbon (C-MIL-125-NH_2)

The as-synthesized MIL-125-NH_2 was heated at 1073 K at a heating rate of 3 K min^{-1} in a tubular furnace under N_2 atmosphere and maintained at this temperature for 2 h. After the carbonization, the yellow powder is converted into a black solid corresponding to C-MIL-125-NH_2.

2.5. Preparation of MOF hybrid membranes (C-MIL-125-NH_2-HM)

C-MIL-125-NH_2 membranes were prepared using a polymer binder (polyvinylidene difluoride, PVDF) and a nylon filter as support adapting a previously reported method (Denny and Cohen, 2015). Basically, 1 g of PVDF/DMF solution (7.5 wt.% PVDF) was added to a vial containing an acetone suspension of C-MIL-125-NH_2 (30 mg carbon/mL acetone). The so obtained mixture was sonicated for 30 min. Afterwards, acetone was evaporated under a stream of nitrogen gas giving rise to a concentrated carbon-PVDF dispersion, which was deposited onto a Nylon filter. Finally, DMF solvent was removed by heating at 333 K for 1 h obtaining a carbon hybrid membrane denoted as C-MIL-125-NH_2-HM. A membrane based on Nylon filter coated with PVDF in the absence of carbon (PVDF/Nylon) was prepared for comparison purposes.

2.6. Batch experiments

The study of the kinetics and the adsorption capacity of the selected phenols of the C-MIL-125-NH_2 was conducted in aqueous solution under batch conditions (adsorbent concentration = 1.0 mg mL^{-1}). Typically, 10 mg of C-MIL-125-NH_2 was added into 10 ml of a 10 mg L^{-1} phenol solution under stirring. The concentration of BPA and 4-tBP left in the supernatants after extraction was determined using UV-Vis spectrophotometry (at a wavelength of 278 nm). Adsorption studies were conducted at

different initial pH values of the phenols solution (pH = 4, 7 and 10) maintaining the solid in contact with the solution during 24 h to ensure the equilibrium conditions. For kinetics experiments, the concentration of remaining pollutant in solution was measured at appropriate time intervals and the sorption data were analyzed with a pseudo-second-order adsorption model, whose linearized-integral form is expressed by the following equation (Ho and McKay, 1999):

$$\frac{t}{q_t} = \frac{1}{k_2 q_2^2} + \frac{t}{q_t}$$

where k_2 is the pseudo-second order rate constant (mg g^{-1} min^{-1}), q_e (mg g^{-1}) is the quantity of phenol adsorbed at equilibrium and q_t (mg g^{-1}) is the phenol sorption at a time of t.

2.7. Solid-phase extraction procedure

The extraction capacity of the prepared hybrid membrane was evaluated using a vacuum filtration system. The membrane was conditioned with 5 mL of acetonitrile followed by 5 mL of water. After a drying step (over 2 min), a 100 mL of a solution of phenol compounds (0.4 mg L^{-1}, each) at pH 7.0 was passed through the membrane at an approximate flow rate of 1 mL min^{-1}, and the non-retained phenols were determined by HPLC of the collected filtrate. For the simultaneous determination of enrichment factors of the mixture of phenols, the collected analytes on the membrane filter were eluted with 5 mL of acetonitrile and the final solution was quantified also with HPLC.

3. Results and discussion

3.1. Preparation of porous C-MIL-125-NH_2

The porous carbon C-MIL-125-NH_2 was obtained by one-step carbonization process under inert atmosphere using only MIL-125-NH_2 MOF as precursor material in the absence of any additional carbon

source. *Figure 1a* shows the powder X-ray diffraction pattern of the precursor MIL-125-NH_2 and that of its derived carbon C-MIL-125-NH_2. The prepared MIL-125-NH_2 crystals showed good crystallinity and the diffraction pattern matched well with that previously reported (Dan-Hardi et al., 2009). After carbonization, the diffraction lines corresponding to the MOF completely disappear, while new diffraction peaks could be observed, which are assigned to titanium oxide particles. The calcination temperature of the MOF determines the formed phase of titanium oxide particles, obtaining in this case a mixture of anatase (JCPDS No. 21-1272) and rutile (JCPDS No. 21-1276), which is consistent with previously reported studies (Guo et al., 2014; Wang et al., 2015). In addition, the XRD pattern of the C-MIL-125-NH_2 exhibited two small broad bands centered around $2\theta = 25$ and 42^{o}, indicating a certain graphitic degree of the obtained carbon (Zhong et al., 2014). According to thermogravimetric analysis performed on C-MIL-125-NH_2 under air (*Figure S1*), the titanium oxide content in the carbon sample is calculated to be 60%. The morphology of the obtained carbon was studied by scanning and transmission electron microscopy. As revealed by SEM images (*figures 1b and S2*), C-MIL-125-NH_2 inherits the disk shape morphology of the precursor MOF (*figure S2*), although the calcination process results in carbon particles with rough surface, smaller diameter, in the range of ~ 1.5 − 2.5 µm, and thickness of around 0.5 µm (Wu et al., 2013; Zhang et al., 2014). Furthermore, TEM micrographs (*figure S3*) revealed that titanium oxide nanoparticles are uniformly distributed in the carbon matrix, which was confirmed by elemental mapping analysis of Ti (*Figure S4*).

Figure 1c shows the nitrogen adsorption and desorption isotherms at 77 K of the prepared C-MIL-125-NH_2, which were analyzed using the BET and 2D-NLDFT methods to examine the textural properties of the obtained carbon. According to IUPAC classification, C-MIL-125-NH_2 exhibits type IV isotherm with a slight hysteresis loop, indicating the coexistence in the sample of micropores and mesopores (Thommes et al., 2015). The BET surface area and total pore volume of the C-MIL-125-NH_2 are 266 $m^2\ g^{-1}$ and 0.16 $cm^3\ g^{-1}$, respectively, which are slightly lower than those of the precursor MIL-

125-NH_2 (Kim et al., 2013) due to a partial collapse of the MOF structure. The pore size distribution (*figure* 1d) confirmed the bimodal porosity of the obtained material, showing that most of the pores have a diameter of 0.9 nm, while a small amount of them have a diameter between 1.4 and 2.4 nm.

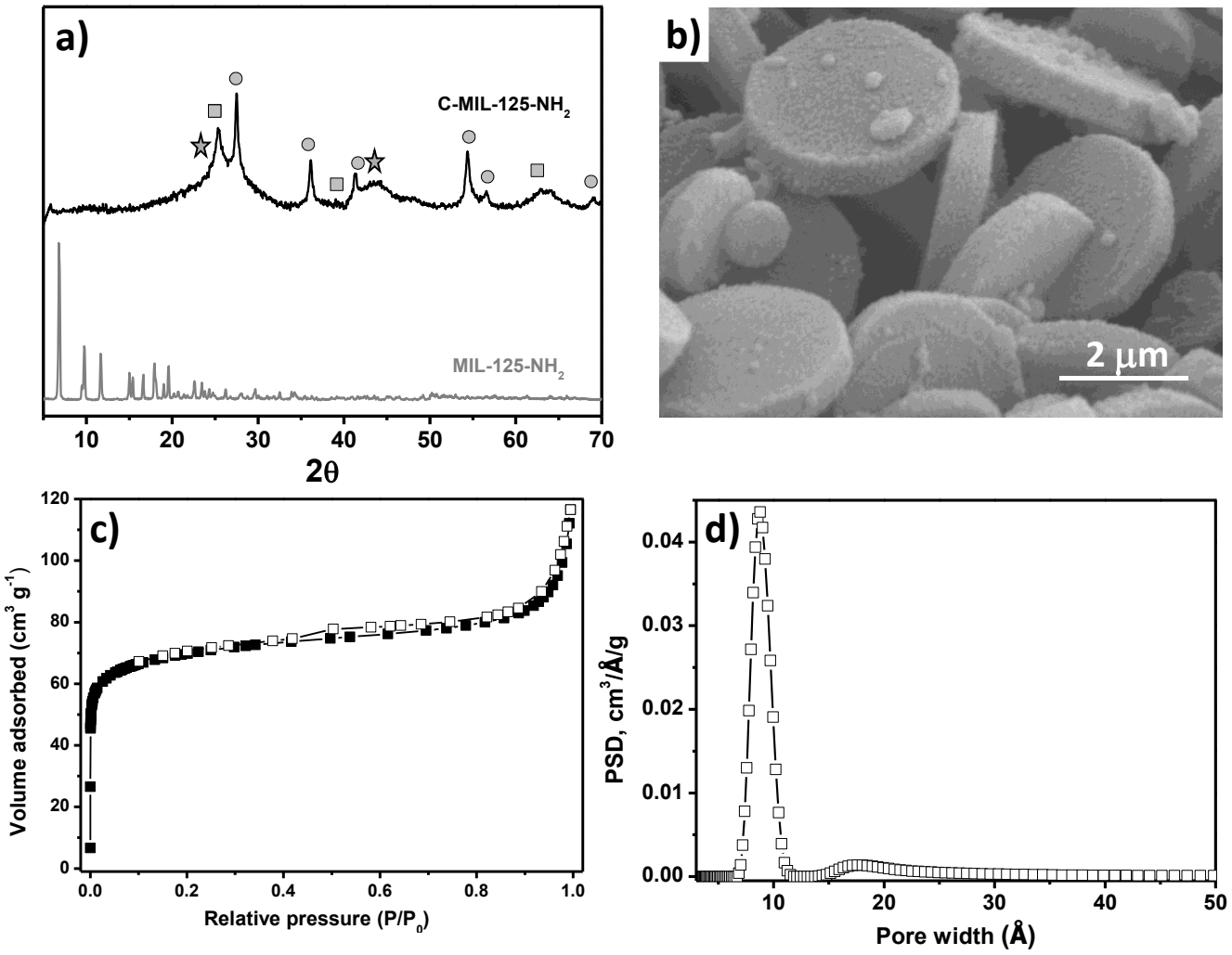

Figure 1. (a) XRD patterns of the MIL-125-NH_2 and the C-MIL-125-NH_2 samples. Peaks: Anatase TiO_2 (squares), rutile TiO_2 (circles), carbon (star). (b) SEM image of the C-MIL-125-NH_2 sample. (c) Nitrogen adsorption-desorption isotherms of the C-MIL-125-NH_2 sample. (d) Pore diameter distribution of the C-MIL-125-NH_2 sample.

3.2. Extraction capacity of the carbon C-MIL-125-NH_2 in batch conditions

The adsorption rate is an important factor to consider in order to use an adsorbent for pollutant extraction. Therefore, kinetics studies were carried out measuring, by UV-visible absorption spectroscopy, the remaining concentration of a 10 mg L^{-1} solution of each pollutant in contact with the adsorbent at predetermined time intervals. The obtained results (*figure 2*) showed that, in both cases, the adsorption data could be fitted by a pseudo-second-order model (Ho and McKay, 1999), obtaining correlation factors of 0.995 and 0.997 for BPA and 4-tBP, respectively. As it can be observed, the adsorption equilibrium was reached in 25 min for BPA and 4-tBP, indicating a rapid extraction in both cases. According to pore size distribution of C-MIL-125-NH_2 (*figure 1d*) and the size of BPA and 4-tBP (Agenson et al., 2003; Nghiem et al., 2008), these pollutants can freely diffuse inside the largest pores of the carbon material, thus facilitating their interaction with the carbon framework. Although in solid-phase extraction, equilibrium conditions are not usually reached, the adsorption isotherms of BPA and 4-tBP were also performed (figure S5). In both cases, the adsorption data well-fitted by Freundlich model (R^2 = 0.96), indicating a multi-layer adsorption (Gonzalez-Serrano et al., 2004; Liu et al., 2017).

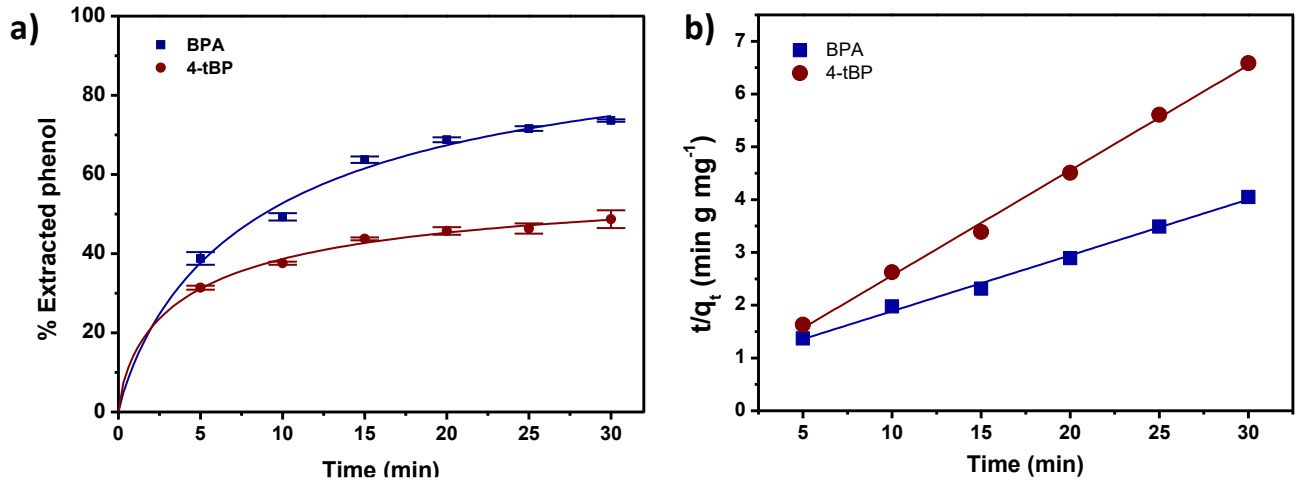

Figure 2. (a) Adsorption capacity of BPA and 4-tBP on C-MIL-125-NH_2 versus time (10 mg C-MIL-125-NH_2; pH 7.0; C_{phenol}, 10 mg L^{-1}). (b) Linear fit of pseudo-second order kinetics model for the adsorption of BPA and 4-tBP on C-MIL-125-NH_2.

In view of the influence of the pH of the extraction medium on the adsorption capacity, as it can change the surface charge of the adsorbent and the chemical speciation in the case of ionizable organic compounds, the adsorption capacity at three pH values of sample solution (4, 7 and 10) was studied. As shown in *figure 3a*, the change of pH from weak acid to neutral (4 to 7) had no significant effect on the extraction capacity of both pollutants, indicating that the adsorptive affinity between the BPA and 4-tBP and the C-MIL-125-NH_2 material is not affected in this range of pH. However, when the solution pH increased from 7 to 10, a significant reduction of the sorption of both phenols was observed. Bearing in mind the pKa value of BPA (9.6) and 4-tBP (10.2) and that the isoelectric point of C-MIL-125-NH_2, determined by the measurement of the zeta potential at different pH values (*figure 3b*), was reached at pH 6.5, the decrease in the extraction capacity of both phenols in basic solutions is due to the electrostatic repulsion between the phenols anions and the negatively charged C-MIL-125-NH_2. The insignificant variation of the adsorption capacity between pH 4.0 and 7.0 indicates that the π-π stacking interactions between the π system of the carbon material and that of the phenol molecules probably is the main sorption mechanisms (Ahmed et al., 2018; Tang, et al., 2016). However, the fact that BPA, a molecule which shows two phenolic rings and hydroxyl groups, was extracted in a higher proportion seems to indicate that other mechanisms such as hydrogen bond could also play an important role.

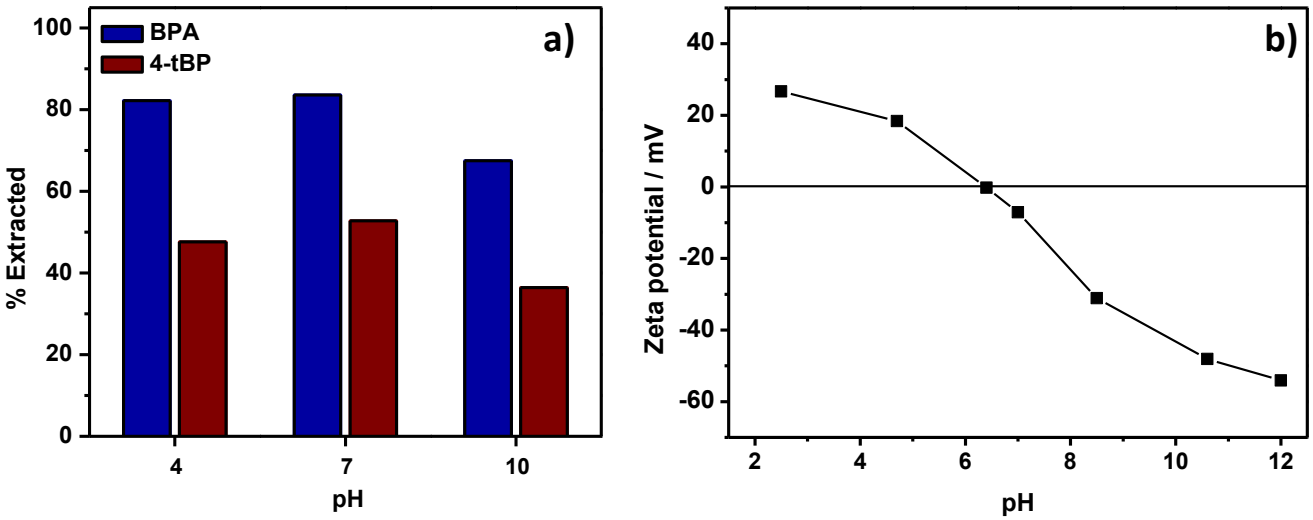

Figure 3. (a) Effect of pH on the adsorption of BPA and 4-tBP (10 mg of C-MIL-125-NH_2; C_{phenol}, 10 mg L^{-1}; time of contact, 24 h. (b) Zeta potential values of C-MIL-125-NH_2 at different pH.

3.2. Characterization of C-MIL-125-NH_2-HM

In order to improve the applicability of the obtained C-MIL-125-NH_2 material and overcome the drawbacks of extraction in dispersive mode, the incorporation of the porous carbon on a functional support was carried out. For that, a simple procedure, based on the coating of a commercially available Nylon filter with a C-MIL-125-NH_2/PVDF suspension, was followed, obtaining a highly robust and apparently homogeneous hybrid membrane as shown in *figure 4a*. SEM micrographs of the hybrid membrane (*figure 4b and S6*) showed that the nylon filter (*figure S7)* is completely covered with a dense layer of C-MIL-125-NH_2 carbon of about 80 µm of thickness, resulting in a membrane of 150 µm of total thickness, as can be observed in the cross-section SEM image of the hybrid material shown in *figure 4c*. Finally, titanium EDS mapping showed the homogeneous distribution of the titanium on the membrane (*figure 4d*) corroborating the uniform deposition of C-MIL-125-NH_2 on the nylon filter.

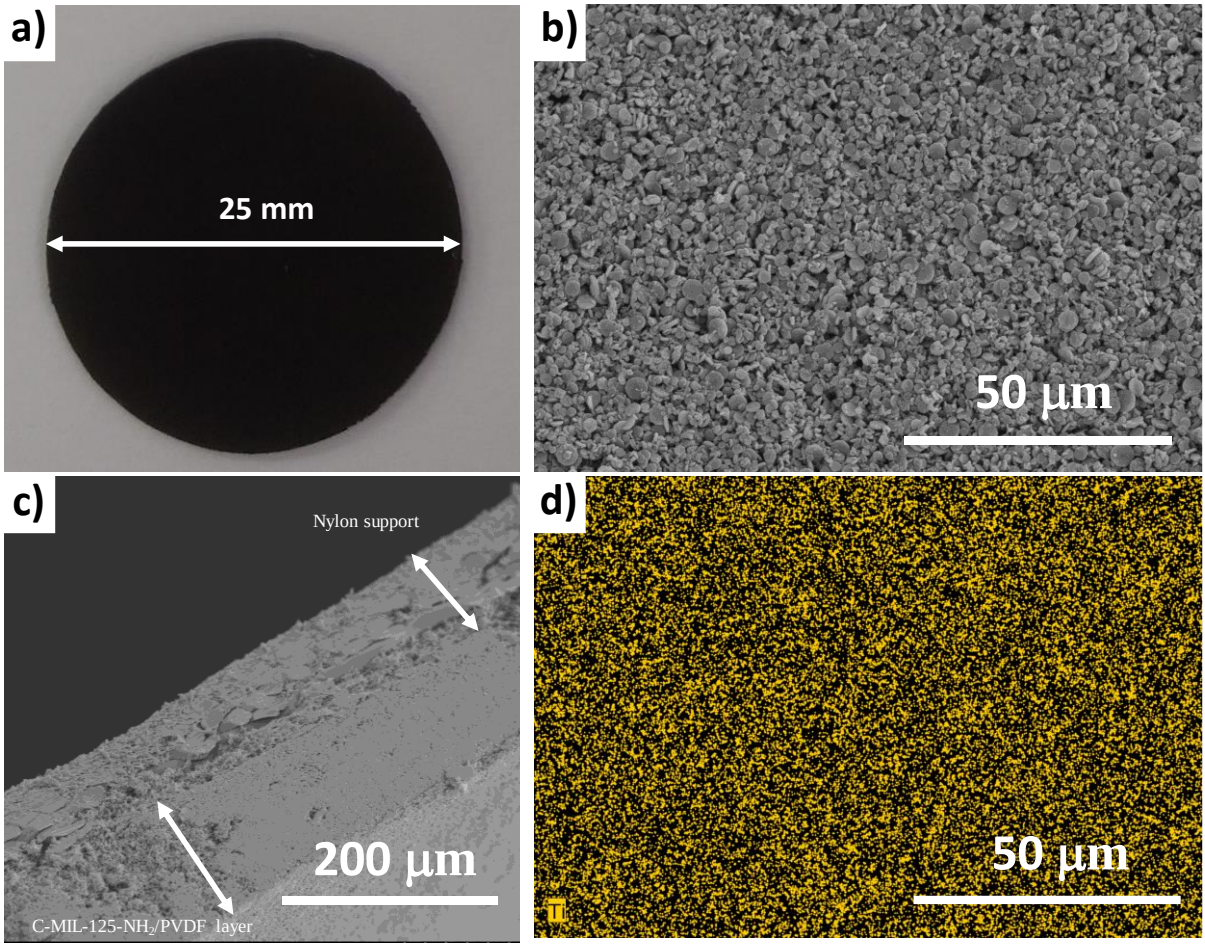

Figure 4. (a) Image of C-MIL-125-NH$_2$-HM. (b) SEM micrograph of C-MIL-125-NH$_2$-HM. (c) Cross-section SEM image of the C-MIL-125-NH$_2$-HM. (d) EDS mapping of Ti of the C-MIL-125-NH$_2$-HM.

3.3. Evaluation of C-MIL-125-NH$_2$-HM in the enrichment of BPA and 4-tBP

To exemplify application of C-MIL-125-NH$_2$-HM, we studied the performance of this composite for the simultaneous extraction and enrichment of low levels of BPA and 4-tBP pollutants from water. *Figure 5a* shows the chromatograms of a standard solution of the two phenols (0.4 mg L^{-1} each) before and after solid-phase extraction using PVDF and C-MIL-125-NH$_2$/PVDF coated membranes. It can be observed that, after direct injection or extraction with a PVDF/Nylon coated membrane, the

corresponding signals for both phenols are very weak, especially when compared with BPA and 4-tBP signals after preconcentration using the membrane coated with the MIL-125-NH_2 derived carbon, which are much more intense than the others, indicating the high preconcentration capability of the prepared hybrid membrane. From these results, enrichment factors were calculated as the ratio of the peak areas obtained from the chromatograms before and after extraction, obtaining values of 109 and 46 for BPA and 4-tBP, respectively. These high values, especially in the case of BPA, demonstrate the feasibility of the developed membrane for extraction and preconcentration of phenols present in water even at low levels.

The C-MIL-125-NH_2-HM was also evaluated for the extraction, under flow conditions, of different volumes of a standard solution of the two phenols. Results are shown in *Figure 5b*. After the filtration of 100 mL of water, the developed hybrid membrane showed high extraction efficiency for both pollutants, achieving an extraction percentage of 100 and 91% for BPA and 4-tBP, respectively. An increase in sample volume (500 mL) resulted in a lower extraction performance of the membrane for both pollutants, however, it still showed a high extraction capacity for BPA (90%), indicating the high ability of the composite to treat high volumes of water polluted with bisphenol A.

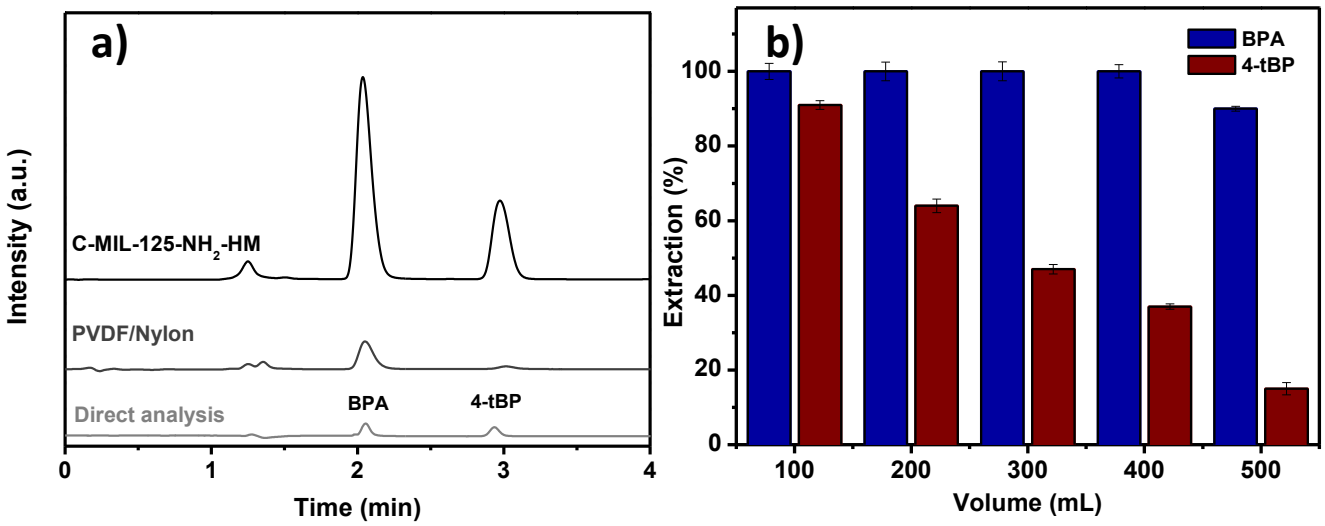

Figure 5. (a) Chromatograms of phenol standard solutions before and after extraction by using PVDF/Nylon and C-MIL-125-NH_2-HM. (b) Extraction of BPA and 4-tBP adsorption on C-MIL-125-NH_2 membrane using different sample volumes.

To gain a deeper insight into the efficiency of the obtained hybrid membrane for the extraction of environmental pollutants, recyclability studies were carried out (*figure 6*). For that, BPA and 4-tBP extraction was repeated 5 consecutive times, washing the membrane with acetonitrile (5 mL) and water (5 mL) between consecutive extractions for its regeneration. After 5 extraction cycles, enrichment factor of the both pollutants practically does not change, being the relative standard deviation of 4.8 and 3.7% for BPA and 4-tBP respectively, which demonstrates the easy regeneration and excellent recyclability of the prepared membrane.

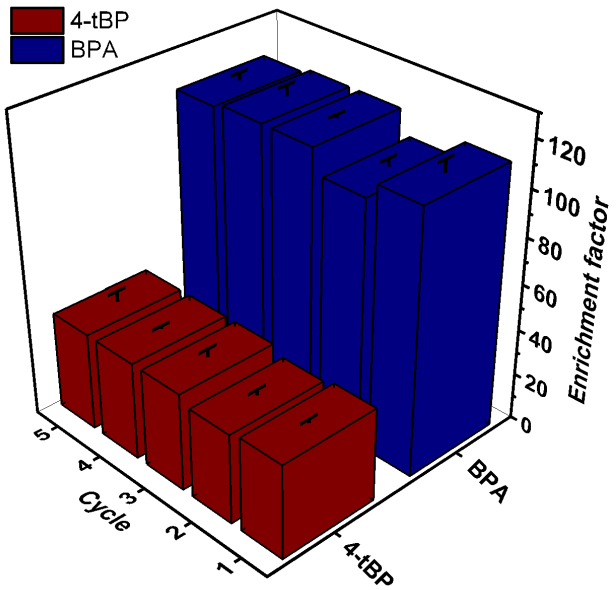

Figure 6. Recyclability of C-MIL-125-NH_2-HM for adsorption of BPA and 4-tBP from water.

3.4. Enrichment of BPA and 4-tBP from well water

As an example of practical application, a groundwater sample was collected from a private well located in Mallorca Island (Spain). BPA and 4-tBP were not detected in the sample and they were spiked with a standard solution of the two phenols (0.4 mg L^{-1}, each). The enriched sample was filtered through the C-MIL-125-NH_2-HM to evaluate the efficiency of the prepared hybrid membrane for the extraction of both pollutants in real samples, testing the potential matrix effect. The pH of the water sample was 7.1. The results for sample analysis are shown in Table 1. In the case of BPA, there is no matrix effect and the membrane allows the complete extraction of the pollutant in both samples. Regarding 4-tBP (less polar compound than BPA), the extraction efficiency was slightly lower in the case of the well water with respect to the ultrapure water. This can be due to the presence of detected ions as nitrate (25.3 mg L^{-1}) and chloride (70 mg L^{-1}). The conductivity value of the sample was 883 µS cm^{-2}. These ions not only impacted the ionic strength, aggrandizing the contact difficulty between the analytes and C-MIL-125-NH_2, but also could occupy the adsorption sites of adsorbent material.

Table 1. Evaluation of the recoveries of BPA and 4-tBP in ultrapure and well water (n=3 replicates)

Water	BPA added (µg L^{-1})	BPA measured after removal (µg L^{-1})	BPA removal (%)	4-tBP added (µg L^{-1})	4-tBP measured after removal (µg L^{-1})	4-tBP removal (%)
Ultrapure water	400	0	100	400	34.4±2.2	91.4
Well water	400	0	100	400	81.8±3.6	79.5

4. Conclusions

In this study, a porous carbon derived from MIL-125-NH_2 MOF by a simple calcination process was prepared, characterized and tested as sorbent of emerging pollutants. The sorptive removal of bisphenol A and 4-tert-butylphenol by C-MIL-125-NH_2 reached equilibrium within 25 min, indicating fast kinetics adsorption of both pollutants. By a simple method using a polymer binder (PVDF), a mechanically stable hybrid membrane of C-MIL-125-NH_2 was prepared. The developed carbon membrane combines the stability and extraction capacity of the C-MIL-125-NH_2 with the good flow-through properties of the membranes, which facilitates its use for the simultaneous extraction and analysis of low levels of mixtures of environmental pollutants in real water samples. In addition, the low-cost of the nylon support and the excellent recyclability of the prepared membrane make it a promising material for water purification.

Acknowledgments

Spanish Agencia Estatal de Investigación (AEI-Spain) and the European Funds for Regional Development (FEDER-European Union) are gratefully acknowledged for financial support through Project CTQ2016-77155-R (AEI/FEDER, UE). N.C. acknowledges the support from the Spanish Ministerio de Educación y Ciencia (FPU pre-doctoral fellowship). L.H. and J.L.G. thank Vicerrectorado de Investigación e Internacionalización of the UIB and Facultad de Ciencias Químicas of the UANL for financial support. The authors acknowledge F. Hierro Riu for scanning and transmission micrographs.

Declarations of interest: none.

Appendix A. Supplementary material

References

Agenson, K.O., Oh, J.I., Urase, T., 2003. Retention of a wide variety of organic pollutants by different nanofiltration/reverse osmosis membranes: controlling parameters of process. J. Membrane Sci. 225, 91–103.

Ahmed, M.B., Zhou, J.L., Ngo, H.H., Johir, M.A.H., Sornalingam, K., 2018. Sorptive removal of phenolic endocrine disruptors by functionalized biochar: Competitive interaction mechanism, removal efficacy and application in wastewater. Chem. Eng. J. 335, 801–811.

An, Y., Zhang, Z., Fei, H., Xiong, S., Ji, B., Feng, J., 2017. Ultrafine TiO_2 Confined in Porous-Nitrogen-Doped Carbon from Metal-Organic Frameworks for High-Performance Lithium Sulfur Batteries. ACS Appl. Mater. Interfaces 9, 12400–12407.

Chaikittisilp, W., Ariga, K., Yamauchi, Y., 2013. A new family of carbon materials: synthesis of MOF-derived nanoporous carbons and their promising applications. J. Mater. Chem. A 1, 14–19.

Chong, M.N., Jin, B., Chow, C.W.K., Saint, C., 2010. Recent developments in photocatalytic water treatment technology: A review. Water. Res. 44, 2997-3027.

Chu, K.H., Al-Hamadani, Y.A.J., Park, C.M., Lee, G., Jang, M., Jang, A., Her, N., Son, A., Yoon, Y., 2017. Ultrasonic treatment of endocrine disrupting compounds, pharmaceuticals, and personal care products in water: A review. Chem. Eng. J. 327, 629–647.

Cui, Y., Li, B., He, H., Zhou, W., Chen, B., Qian, G., 2016. Metal-organic frameworks as platforms for functional materials. Acc. Chem. Res. 49, 483–493.

Dan-Hardi, M., Serre, C., Frot, T., Rozes, L., Maurin, G., Sanchez, C., Férey, G., 2009. A new photoactive crystalline highly porous titanium(IV) dicarboxylate. J. Am. Chem. Soc. 131, 10857–10859.

Denny, M.S., Cohen, S.M., 2015. In situ modification of metal-organic frameworks in mixed-matrix membranes. Angew. Chem. Int. Ed. 54, 9029–9032.

Dhaka, S., Kumar, R., Deep, A., Kurade, M.B., Ji, S.W., Jeon, B.H., 2019. Metal-organic frameworks (MOFs) for the removal of emerging contaminants from aquatic environments. Coord. Chem. Rev. 380, 330–352.

Freyria, F., Geobaldo, F., Bonelli, B., 2018. Nanomaterials for the abatement of pharmaceuticals and personal care products from wastewater. Appl. Sci. 8, 170.

Ghani, M., Picó, M.F.F., Salehiniam, S., Cabello, C.P., Maya, F., Berlier, G., Saraji, M., Cerdà, V., Palomino, G.T., 2017. Metal-organic framework mixed-matrix disks: Versatile supports for automated solid-phase extraction prior to chromatographic separation. J. Chromatogr. A 1488, 1–9.

Gonzalez-Serrano, E., Cordero, T., Rodriguez-Mirasol, J., Cotoruelo, L., Rodriguez, J.J., 2004. Removal of water pollutants with activated carbons prepared from H_3PO_4 activation of lignin from kraft black liquors. Water Res. 38, 3043–3050.

Guo, Z., Cheng, J.K., Hu, Z., Zhang, M., Xu, Q., Kang, Z., Zhao, D., 2014. Metal-organic frameworks (MOFs) as precursors towards TiO_x/C composites for photodegradation of organic dye. RSC Adv. 4, 34221–34225.

371 Hasan, Z., Jhung, S.H., 2015. Removal of hazardous organics from water using metal-organic
372 frameworks (MOFs): Plausible mechanisms for selective adsorptions. J. Hazard. Mater. 283,
373 329–339.

374 Ho, Y.S., McKay, G., 1999. Pseudo-second order model for sorption processes. Process Biochem. 34,
375 451–465.

376 Joseph, L., Zaib, Q., Khan, I.A., Berge, N.D., Park, Y.G., Saleh, N.B., Yoon, Y., 2011. Removal of
377 bisphenol A and 17α-ethinyl estradiol from landfill leachate using single-walled carbon
378 nanotubes. Water Res. 45, 4056–4068.

379 Kim, S.N., Kim, J., Kim, H.Y., Cho, H.Y., Ahn, W.S., 2013. Adsorption/catalytic properties of MIL-125
380 and NH_2-MIL-125. Catal. Today 204, 85–93.

381 Lee, J., Kim, J., Hyeon, T., 2006. Recent progress in the synthesis of porous carbon materials. Adv.
382 Mater. 18, 2073–2094.

383 Li, Y.N., Chen, Z.Y., Bao, S.J., Wang, M.Q., Song, C.L., Pu, S., Long, D., 2018. Ultrafine TiO_2
384 encapsulated in nitrogen-doped porous carbon framework for photocatalytic degradation of
385 ammonia gas. Chem. Eng. J. 331, 383–388.

386 Li, X., Chu, S., Fu, S., Ma, L., Liu, X., Xu, X., 2005. Off-line concentration of bisphenol A and three
387 alkylphenols by SPE then on-line concentration and rapid separation by reverse-migration
388 micellar electrokinetic chromatography. Chromatographia 61, 161–166.

389 Liu, B., Shioyama, H., Jiang, H., Zhang, X., Xu, Q., 2010. Metal-organic framework (MOF) as a template
390 for syntheses of nanoporous carbons as electrode materials for supercapacitor. Carbon 48, 456–
391 463.

Liu, G., Li, L., Xu, D., Huang, X., Xu, X., Zheng, S., Zhang, Y., Lin, H., 2017. Metal-organic framework preparation using magnetic graphene oxide-β-cyclodextrin for neonicotinoid pesticide adsorption and removal. Carbohydr Polym. 175, 584–591.

Ma, J., Liu, W., Liang, X., Quan, B., Cheng, Y., Ji, G., Meng, W., 2017. Nanoporous TiO_2/C composites synthesized from directly pyrolysis of a Ti-based MOFs MIL-125(Ti) for efficient microwave absorption. J. Alloys Compd. 728, 138–144.

Meek, S.T., Greathouse, J.A., Allendorf, M.D., 2011. Metal-Organic Frameworks: A rapidly growing class of versatile nanoporous materials. Adv. Mater. 23, 249–267.

Nghiem, L.D., Vogel, D., Khan, S., 2008. Characterising humic acid fouling of nanofiltration membranes using bisphenol A as a molecular indicator. Water Res. 42, 4049–4058.

Pan, B., Lin, D., Mashayekhi, H., Xing, B., 2008. Adsorption and hysteresis of bisphenol A and 17α-ethinyl estradiol on carbon nanomaterials. Environ. Sci. Technol. 42, 5480–5485.

Park, H.S., Koduru, J.R., Choo, K.H., Lee, B., 2015. Activated carbons impregnated with iron oxide nanoparticles for enhanced removal of bisphenol A and natural organic matter. J. Hazard. Mater. 286, 315–324.

Poole, C.F., 2003. New trends in solid-phase extraction. TrAC Trends Anal. Chem. 6, 362–373.

Ragab, D., Gomaa, H.G., Sabouni, R., Salem, M., Ren, M. Zhu, J., 2016. Micropollutants removal from water using microfiltration membrane modified with ZIF-8 metal organic frameworks (MOFs). Chem. Eng. J. 300, 273–279.

411 Rivera-Utrilla, J., Sánchez-Polo, M., Ferro-García, M.A., Prados-Joya, G., Ocampo-Pérez, R., 2013.
412 Pharmaceuticals as emerging contaminants and their removal from water. A review.
413 Chemosphere 93, 1268–1287.

414 Rowsell, J.L.C., Yaghi, O.M., 2004. Metal-organic frameworks: a new class of porous material.
415 Microporous Mesoporous Mater. 73, 3–14.

416 Shi, X., Liu, S., Tang, B., Lin, X., Li, A., Chen, X., Zhou, J., Ma, Z., Song, H., 2017. SnO_2/TiO_2
417 nanocomposites embedded in porous carbon as a superior anode material for lithium-ion batteries.
418 Chem. Eng. J. 330, 453–461.

419 Tang, L., Xie, Z., Zeng, G., Dong, H., Fan, C., Zhou, Y., Wang, J., Deng, Y., Wang, J., Wei, X., 2016.
420 Removal of bisphenol A by iron nanoparticle-doped magnetic ordered mesoporous carbon. RSC
421 Adv. 6, 25724–25732.

422 Thommes, M., Kaneko, K., Neimark, A.V., Olivier, J.P., Rodriguez-Reinoso, F., Rouquerol, J., Sing,
423 K.S.W., 2015. Physisorption of gases, with special reference to the evaluation of surface area and
424 pore size distribution (IUPAC Technical Report). Pure Appl. Chem. 87, 1051–1069.

425 Wang, P., Lang, J., Liu, D., Yan, X., 2015. TiO_2 embedded in carbon submicron-tablets: synthesis from
426 a metal-organic framework precursor and application as a superior anode in lithium-ion batteries.
427 Chem. Commun. 51, 11370–11373.

428 Wang, T., Wang, J., Zhang, C., Yang, Z., Dai, X., Cheng, M., Hou, X., 2015. Metal-organic framework
429 MIL-101(Cr) as a sorbent of porous membrane-protected micro-solid-phase extraction for the
430 analysis of six phthalate esters from drinking water: a combination of experimental and
431 computational study. Analyst 140, 5308–5316.

Wang, Y., Zhao, H., Zhao, G., 2015. Iron-copper bimetallic nanoparticles embedded within ordered mesoporous carbon as effective and stable heterogeneous Fenton catalyst for the degradation of organic contaminants. Appl. Catal. B: Environ. 164, 396–406.

Wu, H.B., Wei, S., Zhang, L., Xu, R., Hng, H.H., Lou, X.W.D., 2013. Embedding sulfur in MOF-derived microporous carbon polyhedrons for lithium-sulfur batteries. Chem. Eur. J. 19, 10804–10808.

Wu, Z., Zhao, D., 2011. Ordered mesoporous materials as adsorbents. Chem. Commun. 47, 3332–3338.

Yan, J., Huang, Y., Miao, Y.E., Tjiu, W.W., Liu, T., 2015. Polydopamine-coated electrospun poly(vinylalcohol)/poly(acrylic acid) membranes as efficient dye adsorbent with good recyclability. J Hazard. Mater. 283, 730–739.

Zeng, G., He, Y., Zhan, L., Pan, Y., Zhang, C., Yu, Z., 2016. Novel polyvinylidene fluoride nanofiltration membrane blended with functionalized halloysite nanotubes for dye and heavy metal ions removal. J. Hazard. Mater. 317, 60–72.

Zhang, L., Su, Z., Jiang, F., Yang, L., Qian, J., Zhou, Y., Li, W., Hong, M., 2014. Highly graphitized nitrogen-doped porous carbon nanopolyhedra derived from ZIF-8 nanocrystals as efficient electrocatalysts for oxygen reduction reactions. Nanoscale 6, 6590–6602.

Zhang, X., Zhang, H., Xiang, Y., Hao, S., Zhang, Y., Guo, R., Cheng, X., Xie, M., Cheng, Q., Li, B., 2018. Synthesis of silver phosphate/graphene oxide composite and its enhanced visible light photocatalytic mechanism and degradation pathways of tetrabromobisphenol A. J. Hazard. Mater. 342, 353–363.

Zhong, H.X., Wang, J., Zhang, Y.W., Xu, W.L., Xing, W., Xu, D., Zhang, Y.F., 2014. ZIF-8 derived Graphene-based nitrogen-doped porous carbon sheets as highly efficient and durable oxygen reduction electrocatalysts. Angew. Chem. Int. Ed. 53, 14235–14239.